

ORIGINAL RESEARCH

Evaluating the Effect LRB Isolators in Retrofitting a Truss Bridge

Moradi M.¹, Rahimi S.^{2,*}, Rezaei S.³, Ranjbar N.⁴

Abstract:

One of the things used to equip and strengthen bridges is the addition of a seismic isolator. In this study, the seismic performance of a truss bridge equipped with a seismic isolator has been evaluated. Thus, two structural models of a truss bridge have been modeled nonlinearly in the Perform software. One is the initial and main model and the other has a seismic isolator. Initially, using incremental dynamic analysis, seismic parameters such as the horizontal displacement of the superstructure, the hysteresis curve and the time history of the moment applied to the column, the horizontal displacement of the column head and the hysteresis curve of the models have been investigated. Finally, the incremental dynamic curves and the fragility of the structures have been investigated and compared using twenty earthquake records. The results show that the use of an isolator reduces the horizontal displacement of the bridge column and reduces the probability of its collapse at different accelerations and different performance levels.

Keywords:

Truss bridge, seismic isolator, seismic performance, fragility curve, retrofitting

✉*Corresponding author Email: Sepideh.rahimi@iau.ac.ir

1 Faculty of Civil Engineering, University of Science and Technology of Mazandaran, Behshahr, Iran (m.moradi@mazust.ac.ir)

2 Department of Civil Engineering, No.C., Azad University, Noor, Iran

3 Faculty of Civil Engineering, University of Science and Technology of Mazandaran, Behshahr, Iran (S.Rezaei@mazust.ac.ir)

4 Department of Civil Engineering, No.C., Azad University, Noor, Iran (Nima.Ranjbar@iau.ac.ir)

1. Introduction

Bridges, as important and key elements in a country's arterial road network, play a unique role economically, politically, and militarily [1]. Bridges are divided into types of wood, masonry, iron, steel, reinforced concrete, prestressed concrete, aluminum bridges, or composite materials according to the materials used. Structural systems of bridges include flat or girder bridges, beam bridges, trusses, and arch or suspension bridges [2]. Truss bridges are one of the oldest types of bridges that are economical due to the optimal use of materials [3]. There is extensive research on the seismic assessment of truss bridges. Mousavi et al. (2020) conducted a study on the damage assessment of a truss bridge [4]. Zhou et al. (2022) examined the behavior of truss bridges in the context of gradual damage [5]. Pham et al. (2023) investigated the retrofitting of truss bridges using CFRP sheets [6]. Zhi et al. (2023) investigated the performance-based retrofitting of long-span truss bridges based on alternative load path redundancy analysis [7]. Suserboram et al. (2019) presented a study on the seismic retrofitting of steel truss bridges using buckling dampers [8].

There are various methods to improve the seismic performance of bridges. The use of seismic isolators is one of these methods that is commonly used in the retrofitting of these structures. Hanay et al. (2018) investigated the retrofitting of truss bridges on roads and railways using seismic isolators [9]. (2020) evaluated the performance-based seismic retrofitting of isolated highway bridges equipped with shape memory alloy cable restraints with different life cycle dimensions [10].

A base seismic isolator is a system that is placed under structures to protect some of the structural components from the destructive effects of ground acceleration [11]. Of course, the use of this equipment does not mean that the structure is completely protected from earthquake damage; rather, by isolating the structure from the ground, the damage caused by large earthquakes is greatly reduced [12]. Types of seismic isolation systems include:

Slip-based, lead-core, elastomeric, friction pendulum, rebound friction bearing (R-FBI), low-damping natural and synthetic rubber, high-damping natural rubber, pure friction, fiber-reinforced elastomeric [13]. Therefore, in this study, an attempt has been made to first evaluate one of the country's bridges under seismic loads. Then, this structure is equipped with a seismic isolator. This isolator is placed between the truss and the columns. First, the seismic performance of the two bridges and then the fragility of the two structures are evaluated. In the following, the

structural model of the case

2. Structural model

The bridge considered for this study is the Takab Bridge (Figure 1). The Takab Bridge is located on the Andimeshk route. The length of this bridge is 228.75 meters and includes two 61-meter side spans and a 106.75-meter middle span. The bridge deck consists of a variable-height metal truss with longitudinal metal beams and a cast-in-place concrete slab that acts as a composite. Its total width is 10 meters, including an 8-meter-wide carriageway and two cornices and sidewalks, each 1 meter wide. The bridge is located on abutments at both ends. The middle piers are in the form of concrete frames. The height of the truss on the pier is 10.9 m and on the abutments is 4.95 m and the connection at the two ends of the bridge is in the form of hinges. The design and control of stresses have been carried out according to the AASHTO [14] code.



Figure 1. Tokab Bridge.

Four reinforced concrete columns were used to build this bridge. Based on the available data, concrete with a compressive strength of 28 MPa and longitudinal reinforcements with a yield stress of 400 MPa were used to build the foundations of this structure. The height of the bridge foundations is 15.32 meters. These foundations have a rectangular cross-section with dimensions of 2 x 1.7 meters and have 130 reinforcements with a diameter of 32. Steel with a yield stress of 370 MPa (St52) was used for the truss. Sections such as

2UNP 320 with two plates with dimensions of 455 mm x 10 mm, an I-shaped sheet beam with a height of one meter, a wing width of 30 cm and a thickness of 3.5 cm were used to build this truss. This bridge was modeled nonlinearly in the Perform software based on the finite element method. Figure (2) presents the finite element model of this bridge before retrofitting. This model is introduced as case 1 in this study. This bridge was built in 2007. The concentrated plastic hinge method was used for nonlinear modeling of this structure. The elements were modeled based on FEMA 356. The modeling parameters and acceptance criteria introduced in this standard were used in the modeling of the elements. For example, to assign nonlinear behavior of axial elements in the PERFORM3D software, the Steel bar/Tie/Strut-Simple Bar element, which is only capable of withstanding axial force, is used. For this purpose, first, in the nonlinear material characteristics section, buckling steel materials with the title Inelastic Steel Material, Buckling have been used. In this type of material, the behavior in tension and compression is different. Figure 2 shows the finite element model of this bridge.

3. Seismic load

In this study, the time history dynamic analysis method has been used to evaluate the dynamic response and performance level of the structure. One of the objectives of this study is to evaluate the fragility of the structure against the applied loads. For this purpose, it is necessary to use incremental dynamic analysis. Twenty records introduced by FEMA P695 have been used to apply the seismic load. Twenty near-field records have been selected and are presented in Table 1. Each of these records has been scaled from a maximum acceleration of 0.1g with steps of 0.1g until the structure reaches the instability limit. A maximum drift criterion of 0.1 has been considered for the instability of the structure.

4. Seismic isolator

In this research, the method provided by the Ashto standard for seismic isolator design has been used [15]. The following steps have been taken for seismic isolator design: 1- Initial assumption for the initial shear stiffness (K_u), secondary stiffness (K_d), yield force (F_y) and maximum displacement of the isolator (d) 2- For each seismic isolator, the effective stiffness (K_{eff}) and the entire isolated structure, which is a combination of the stiffness of all isolators and the stiffness of the substructure (K_{sub}), are calculated 3- Calculation of the effective period of the entire isolated structure using the parameters of the damping coefficient C , the total weight of the structure W , the acceleration due to gravity g , the acceleration coefficient A and the site coefficient S_i . 4- Calculate the equivalent viscous damping 5- Given the equivalent viscous damping, determine the coefficient C from the Ashto table. 6- Compare the value of the coefficient C in steps 3 and 5 7- If the value of the coefficient C in the two above steps is different, the values of d are changed and the above steps are repeated.

1. Fragility Analysis

In general, the fragility curve is defined as equation 1:

$$\text{Fragility} = P[\text{EDP} > \text{AC} | \text{IM}] \quad (1)$$

In the above equation, IM is the earthquake intensity, which is usually assumed to be equal to the maximum ground acceleration (PGA), spectral acceleration (S_a) or spectral displacement (S_d), EDP is the engineering demand parameter, which is obtained from the analysis output, and AC is the acceptable condition corresponding to the assumed limit state [19]. A statistical distribution is considered for each engineering demand parameter (EDP) at each earthquake motion intensity (IM). To evaluate the probability of exceeding a specific boundary limit (AC), the mean and standard deviation of each of the EDPs are calculated for the effect of the sum of the earthquake maps. Then, using an appropriate distribution function, the probability of each of the EDPs exceeding the given limit state is calculated.

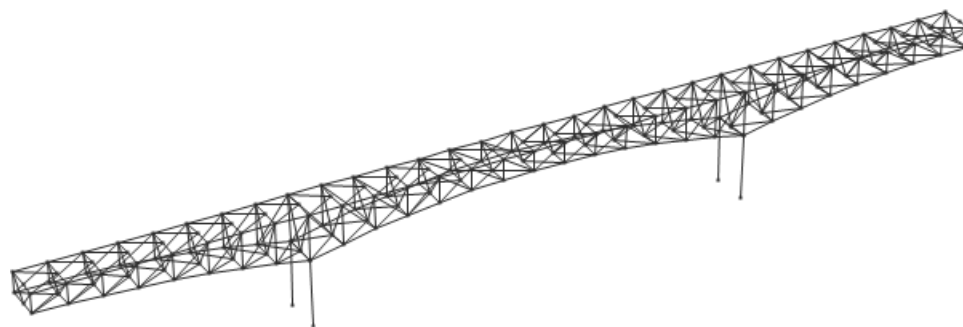


Figure 2. Finite element model of Tokab Bridge.

Table 1. Seismic loads [17, 16]

ID No.	Lowest Freq (Hz.)	PEER.NGA Record information	PGAm _{ax} (g)
1	0.13	IMPVALL/H-E06_233	0.44
2	0.13	IMPVALL/H-E07_233	0.46
3	0.16	ITALY/A-STU_223	0.31
4	0.15	SUPERST/B-PTS_037	0.42
5	0.13	LOMAP/STG_038	0.38
6	0.13	ERZIKAN/ERZ_032	0.49
7	0.07	CAPEMEND/PET_260	0.63
8	0.10	LANDERS/LCN_239	0.79
9	0.11	NORTHR/RRS_032	0.87
10	0.12	NORTHR/SYL_032	0.73
11	0.13	KOCAELI/IZT_180	0.22
12	0.08	CHICHI/TCU065_272	0.82
13	0.06	CHICHI/TCU102_278	0.29
14	0.10	DUZCE/DZC_172	0.52
15	0.06	GAZLI/GAZ_177	0.71
16	0.13	IMPVALL/H-BCR_233	0.76
17	0.06	IMPVALL/H-CHI_233	0.28
18	0.13	NAHANNI/S2_070	0.45
19	0.13	LOMAP/BRN_038	0.64
20	0.25	LOMAP/CLS_038	0.51

Therefore, for better evaluation of the results, an appropriate probability distribution should be used. One of the common distributions in the fragility curve scenario is the normal distribution function [17].

6. Dynamic response

There are many parameters for evaluating the dynamic response of structures, and an attempt has been made to address a large number of them in this study to determine to what extent the use of a lead core type seismic

isolator can affect the dynamic performance and dynamic response, as well as the performance of this bridge. One of the important parameters in evaluating the dynamic response of bridges is to examine the horizontal displacement of the bridge superstructure. Therefore, the displacement of the middle point in the two bridges has been evaluated. Figure 3 presents the horizontal displacement curves at the middle point of the Takab Bridge in two cases with and without the isolator under the Tebes earthquake record

using incremental dynamic analysis at multiple maximum accelerations (PGA).

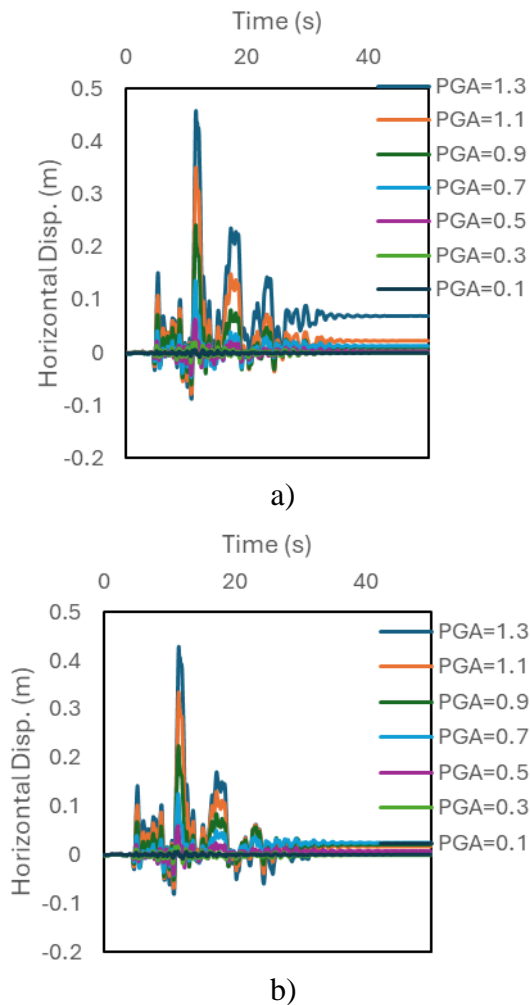


Figure 3. Time history curves of the horizontal displacement of the bridge superstructure under the Tebes earthquake record a) Isolated structure b) Initial structure.

Usually, in the evaluation of horizontal displacement as a dynamic response of structures, two important components are considered. One of these two parameters is the maximum displacement and the other is the permanent displacement [20]. The greater the horizontal displacement in the structure, the greater the dynamic response the structure has endured, and the greater the residual displacement in the structure, the greater the amount of permanent deformation in the structure, which results in greater structural damage [21-27].

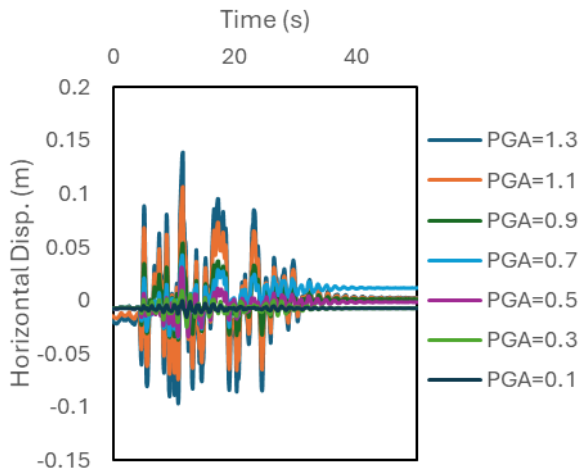
Studies of the time history curves of horizontal displacement of bridges show that the horizontal displacement in the isolated

bridge is slightly greater than the original structure at most maximum accelerations. Meanwhile, at a maximum acceleration of 1.3g, the permanent displacement in the structure with seismic isolation is greater than the original structure. The maximum horizontal displacement values in the superstructure of the bridge with seismic isolation at maximum accelerations of 0.1, 0.3, 0.5, 0.7, 0.9, 1.1 and 1.3g are calculated to be 0.006, 0.019, 0.06, 0.13, 0.24, 0.34 and 0.45 m, respectively. These values in the original structure are calculated to be 0.006, 0.018, 0.05, 0.12, 0.22, 0.33 and 0.42 m, respectively. These values indicate that the displacement in the superstructure of the bridge with seismic isolation is greater than that in the original structure.

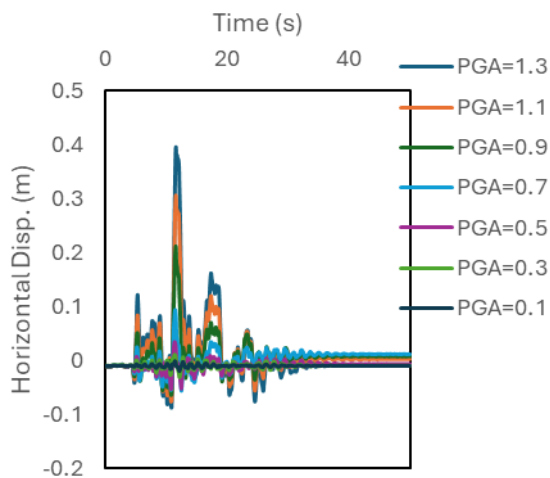
The main role of the seismic isolation in bridges is to reduce the transmission of vibrations from the superstructure to the bridge columns to reduce column damage. Therefore, it should be determined how much the displacement difference is in the columns of the two bridges. Figure 4 presents the time history curves of the horizontal displacement of the head of one of the columns of the two structures under the record of the Tebes earthquake at different maximum accelerations.

Examination of the time history curves of the horizontal displacement of the column heads shows that the horizontal displacement pattern in the original bridge column is similar to the horizontal displacement in the bridge superstructure. However, the displacement pattern of the column head in the structure with the isolator bridge is completely different from the horizontal displacement of the bridge superstructure. This shows that the seismic isolator has been able to play its role in reducing the vibrations of the bridge columns properly. The maximum horizontal displacement values at the top of the column of the bridge with seismic isolator at maximum accelerations of 0.1, 0.3, 0.5, 0.7, 0.9, 1.1 and 1.3g have been calculated to be 0.00013, 0.009, 0.03, 0.04, 0.05, 0.1 and 0.14 m respectively.

These values in the original structure have been calculated to be 0.001, 0.01, 0.03, 0.09, 0.21, 0.3 and 0.39 m respectively. This shows that firstly, the displacement values at the top of the column are less than the displacement of the superstructure. Second, the use of seismic isolator has significantly reduced the maximum displacement experienced by the column.



a)



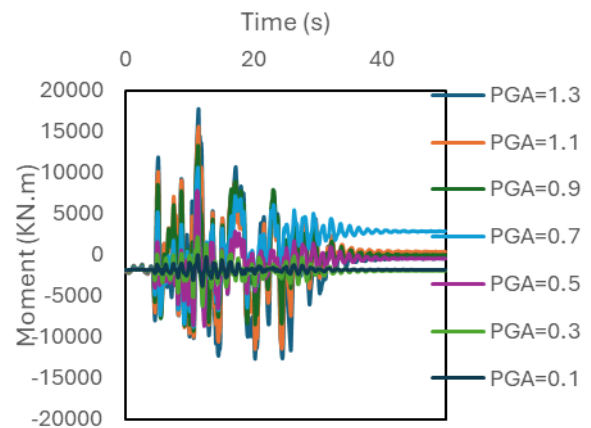
b)

Figure 4. Time history curves of horizontal displacement of the bridge column head under the record of the Thebes earthquake. a) Isolated structure b) Initial structure.

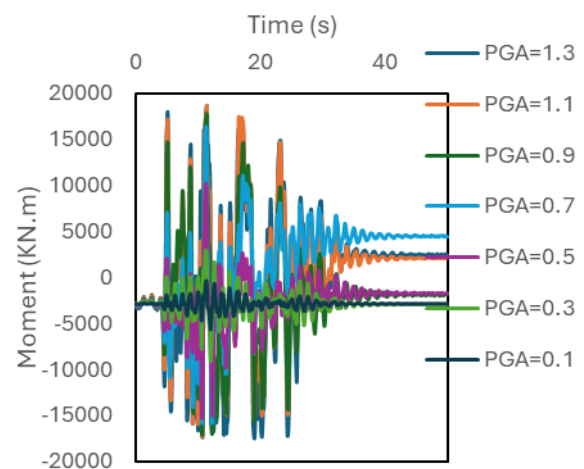
Now it should be examined whether this reduction in displacement also leads to a reduction in the applied moment to the columns. For this purpose, Figure 5 presents the time history curves of the applied moment to one of the four columns of the structure

under the record of the Thebes earthquake at different maximum accelerations.

Examination of the time history curves of the two bridges with and without isolators shows that the maximum values of the applied moment to the column of the isolated structure are less than the structure without isolators.



a)



b)

Figure 5. Bridge column moment time history curves under the Thebes earthquake record: a) Isolated structure b) Initial structure.

The maximum values of the applied moment to the column of the bridge with seismic isolators at maximum accelerations of 0.1, 0.3, 0.5, 0.7, 0.9, 1.1 and 1.3g are calculated to be 3830, 6324, 8585, 10552, 13280, 15561 and 17633 kNm, respectively. These values in the original structure were calculated to be

5612, 9150, 15244, 16400, 17836, 18639, and 18688 kNm, respectively. As is clear, the maximum moment acting on the columns of this bridge in the two cases of isolator and without it is completely different from each other, and the bridges with the seismic isolator structure experienced much lower moment values than the original structure. The time history curve of the applied moment to the column does not provide the ability to show how much the element has entered a nonlinear state. Therefore, it is better to examine the hysteresis curves of the columns of the two structures. Figure 6 shows the hysteresis curves of the two columns of the structure under the Thebes earthquake record for different maximum accelerations.

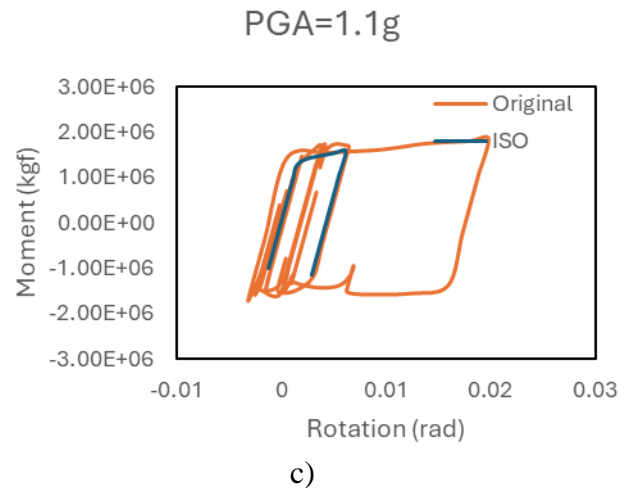
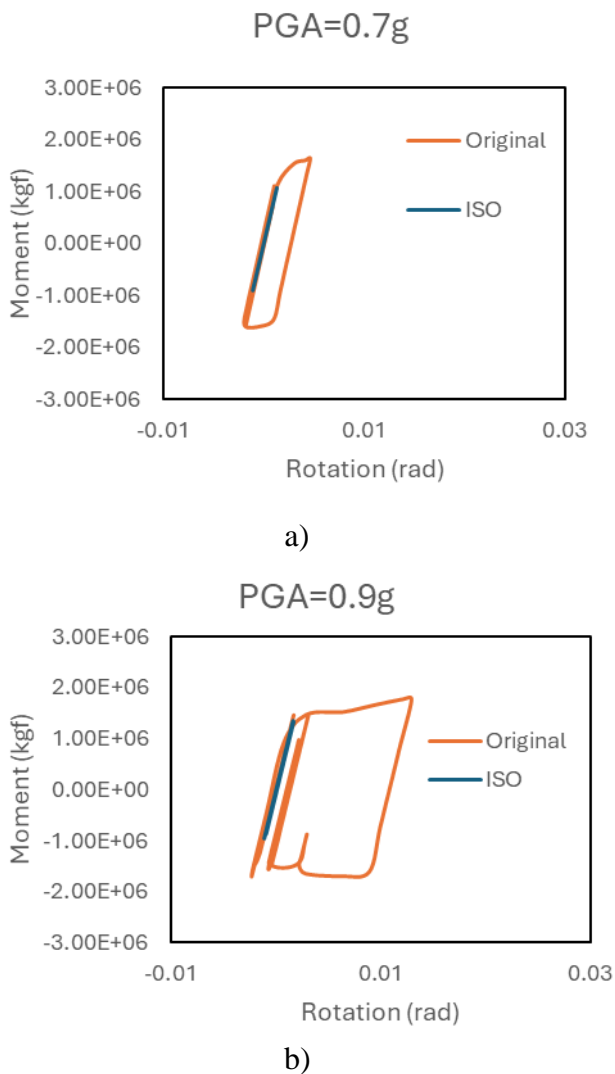


Figure 6. Hysteresis curves of one of the four bridge columns under the Thebes earthquake record a)0.7g b)0.9g c)1.1g

The hysteresis curve can remain in the linear region or enter the nonlinear region based on the amount of applied load. At a maximum acceleration of 0.7 g, the bridge column of the original structure has entered the nonlinear region, but the column of the structure with seismic isolation still remains in the linear region.

At maximum accelerations greater than 0.7 g, the column of the structure with seismic isolation has entered the nonlinear region, but its width is much less than that of the original structure, which means that the damage that the column in the original structure receives is greater than the damage that the column in the structure with seismic isolation receives. Up to this part of the study of the dynamic response of the structure, it has been determined that the dynamic response of the structure above the bridge with seismic isolation is greater than that of the original structure, but the dynamic response of the structure below, that is, the columns in the original bridge, is greater than that of the isolated structure.

Now it is necessary to examine how much effect the use of seismic isolators had on the overall performance of the bridge. The best criterion for this is to examine the performance levels of the two structural members.

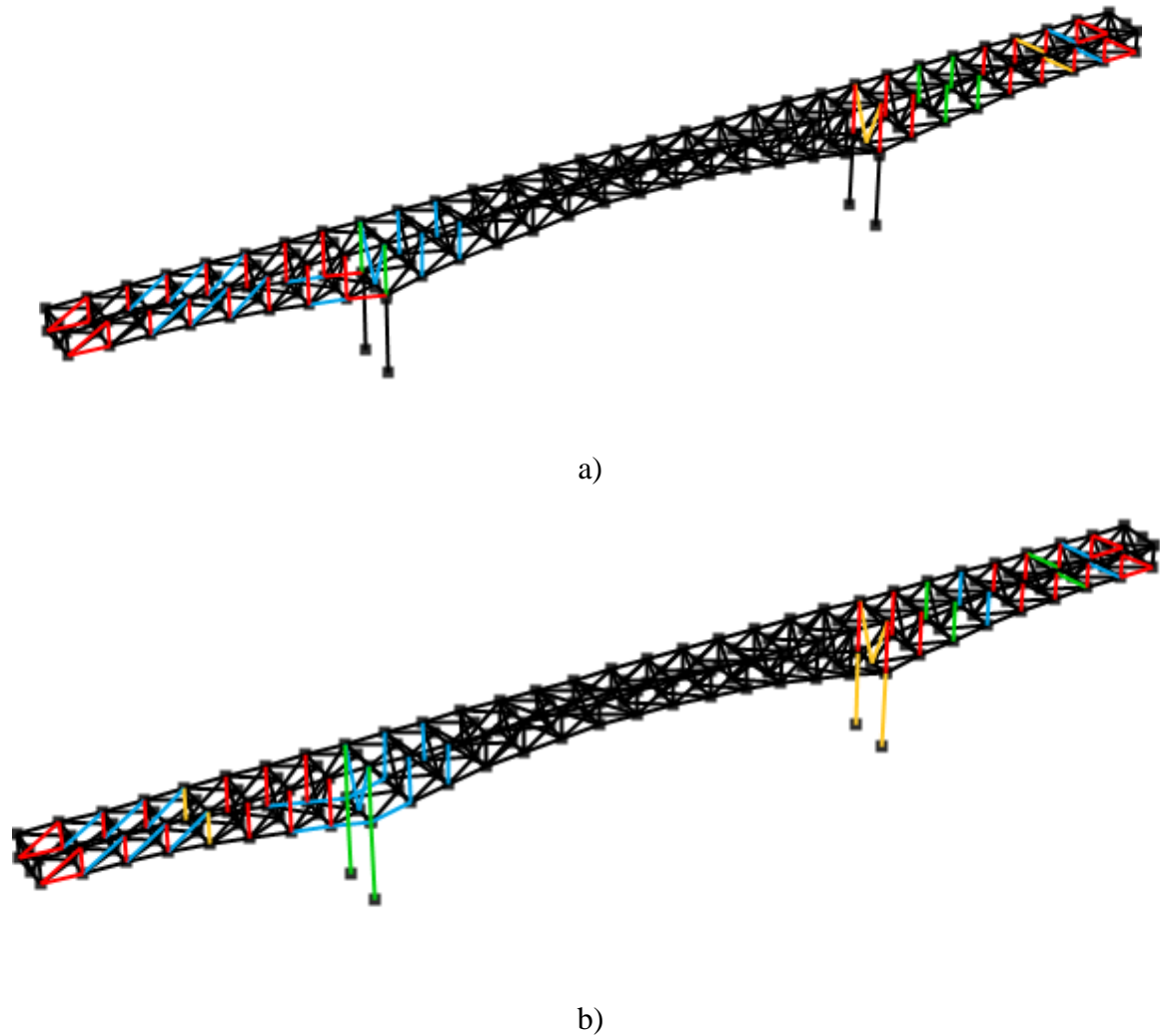


Figure 7. Performance of structural elements in the Tebes earthquake record with a maximum acceleration of 1.1 g. a) Structure with seismic isolator b) Initial structure.

Figure 7 shows the performance levels of the structural elements at the maximum acceleration of 1.1 g recorded in the Tebes earthquake.

The performance of the two structures at a maximum acceleration of $g1.1$ indicates that although two of the four columns in the main structure are on the verge of reaching the LS performance level, the columns of the structure with seismic isolation still remain far from the LS zone and in the safe zone. However, the structure with seismic isolation has a greater number of elements in the superstructure section that have reached the LS performance level. Figure 8 presents the performance levels in the LS zone for the two

structures under the record of the Tebes earthquake with a maximum acceleration of $g1.3$.

The same trend as that stated for the maximum acceleration of $g1.1$ is also evident for the maximum acceleration of $g1.3$. The difference is that at this maximum acceleration, two columns in the original structure have reached the LS performance level, but the columns of the isolated structure have remained within the safe range. Also, in the superstructure section, the number of elements that have reached the LS performance level in the structure with a seismic isolator is greater than in the original structure.

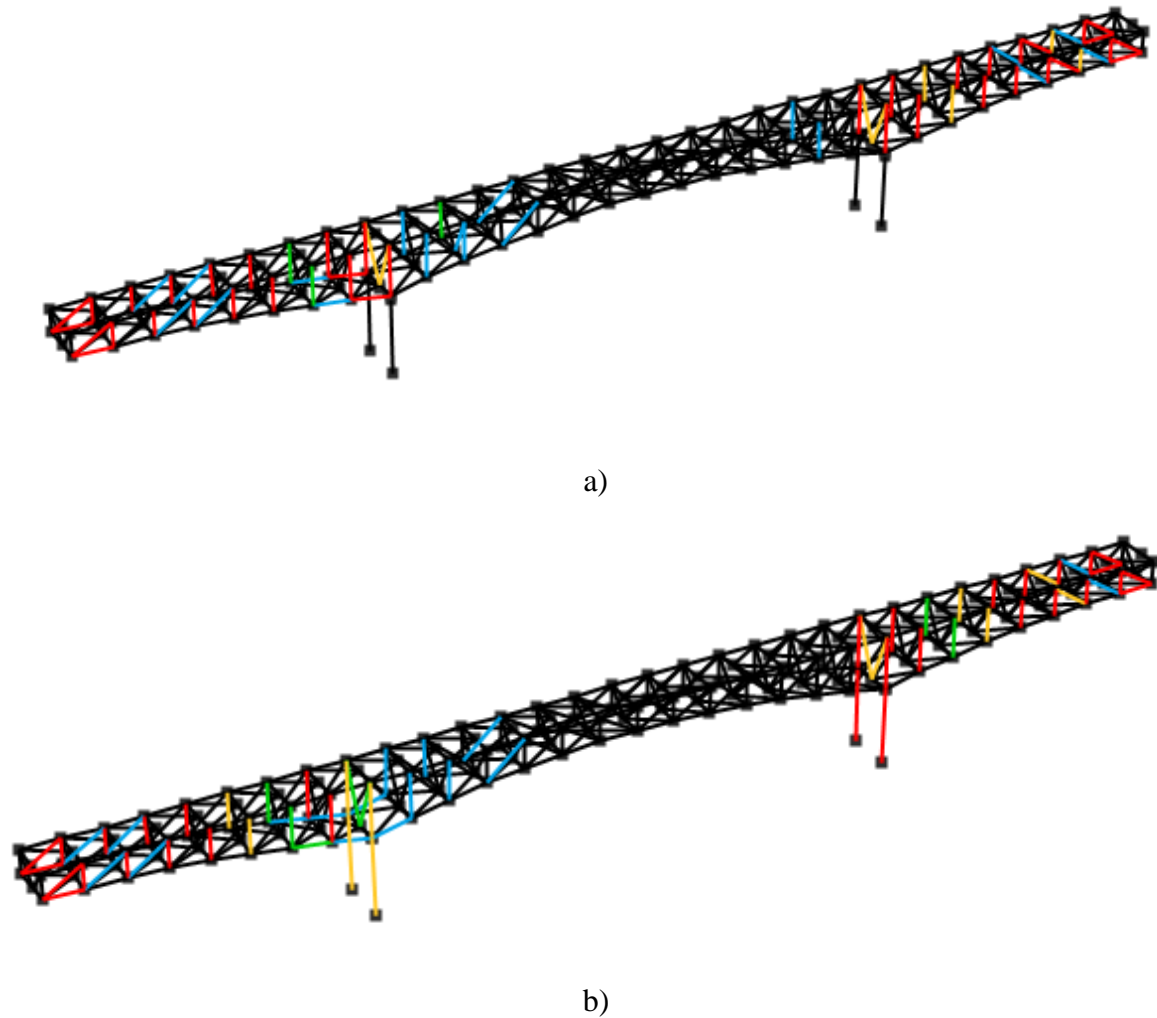


Figure 8. Performance of structural elements in the Thebes earthquake record with a maximum acceleration of 1.3 g a) Structure with seismic isolation b) Initial structure

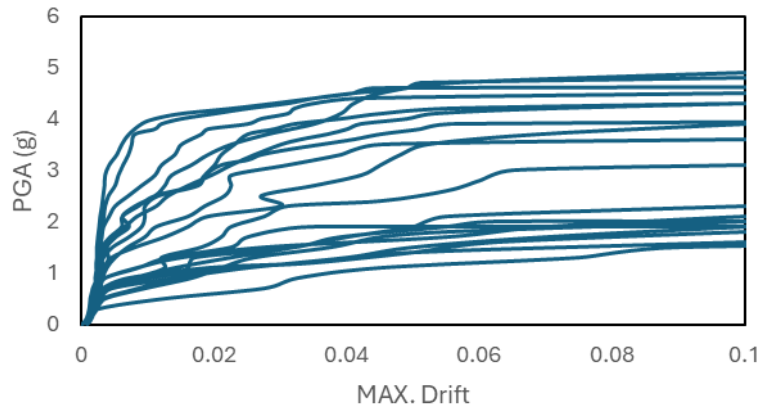
Therefore, it can be concluded that the use of a seismic isolator, although it can reduce the horizontal displacement and the amount of moment in the column below it to an acceptable extent, increases the displacement and increases the performance level in the superstructure section.

7. IDA and fragility curves

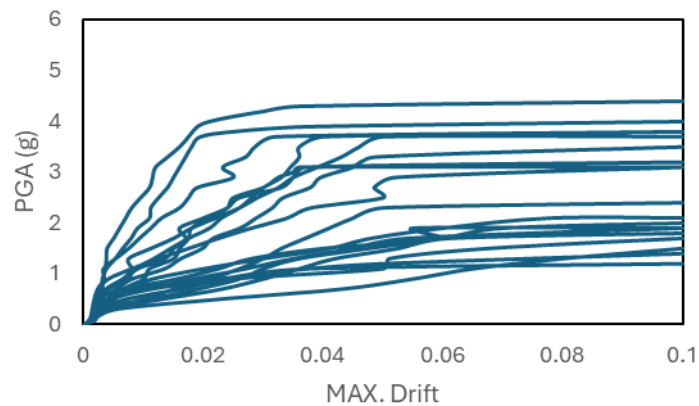
In Section 6, an attempt has been made to comprehensively examine the dynamic response and performance of the Takab Bridge with and without a seismic isolator. In this section, an attempt has been made to examine the IDA curves and then the fragility curves of these two bridges together using incremental dynamic analyses. Figure 9

presents the IDA curves of the original Takab Bridge and the Takab Bridge with seismic isolation.

As mentioned, the effect of using a seismic isolator is to reduce vibrations and deformations of bridge columns. In the previous section, it was shown to what extent a seismic isolator can reduce the displacement and moment values applied to the structural column. In this section, the 20 records introduced in Table (1) are applied incrementally to bridges with seismic isolators and the original Takab bridge. The maximum drift of Takab bridge columns in two cases is extracted and presented as IDA curves for each record in Figure 9.



a)



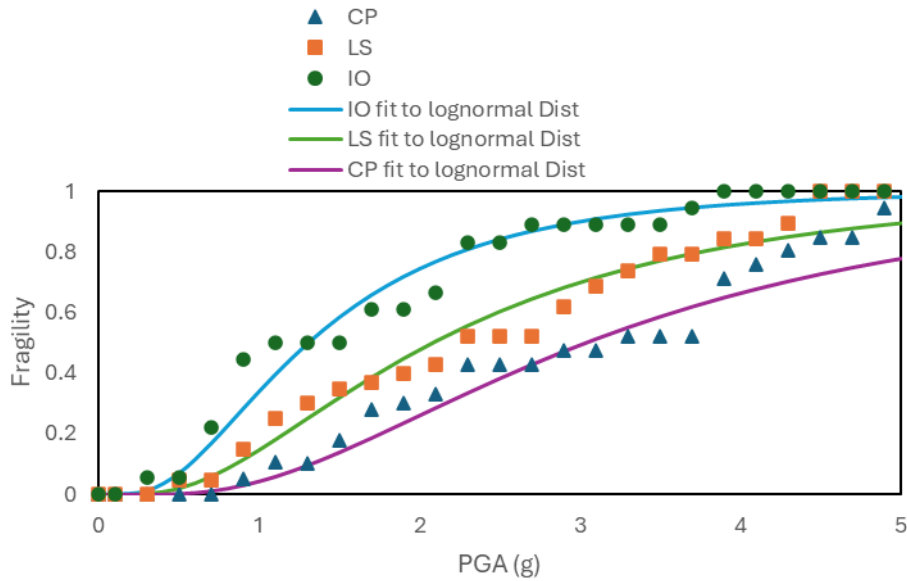
b)

Figure 9. IDA curves of Takab Bridge in the case of a) with separator b) initial structure

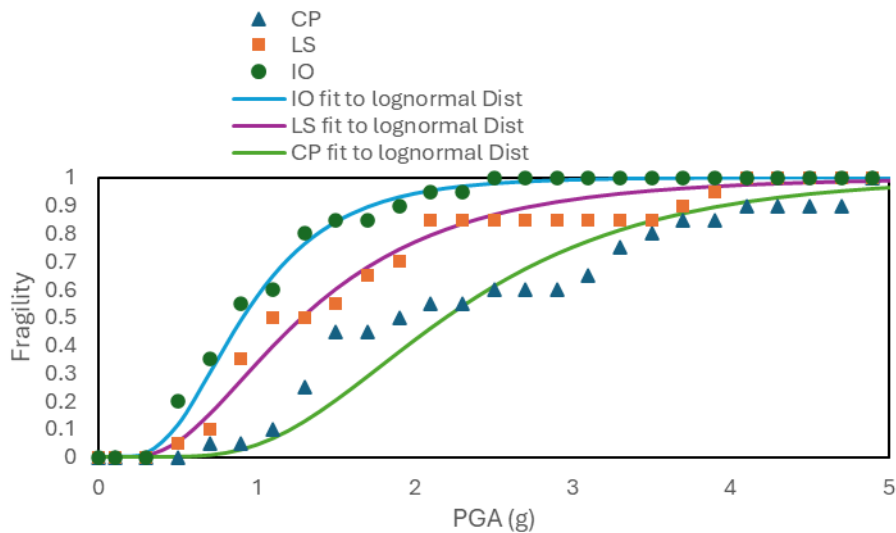
The application of IDA curves is in the evaluation of fragility curves. Fragility curves provide the probability of structural failure at different performance levels. Three levels IO, LS and CP have been used in the evaluation of fragility curves of Takab bridge columns. To determine the probability of exceeding the three mentioned levels, the values 0.01, 0.02 and 0.04 are considered as the drift of the IO, LS and CP limits. Figure 10 presents the fragility curves of two structures from the mentioned levels. In this figure, the points

indicate the probability of the column exceeding the desired performance levels, which are obtained directly from the twenty mentioned records, and the lines are the probability values that are aligned with these points.

The fracture curves of the Takab Bridge column in the initial and isolated states show that the use of an isolator can reduce the probability of failure at three performance levels.



a)



b)

Figure 10. Fragility curves of the Takab Bridge in the case of a) with separators and b) the initial structure.

For example, at the IO performance level, the probability of failure at maximum acceleration g_1 for the column of the isolated structure and the initial structure is calculated to be 0.4 and 0.63, respectively. These values for the LS levels are calculated to be 0.18 and 0.39, respectively. Also, the probability of

failure at the CP level at maximum acceleration g_2 for the column of the isolated structure and the initial structure is calculated to be 0.33 and 0.46, respectively.

8. Conclusion

The aim of this research was to investigate the seismic performance and dynamic response of

the Takab truss bridge in two states with and without a seismic isolator. Initially, a nonlinear model of the main structure of this bridge, that is, without a seismic isolator, was created in the Perform software. Then, according to the specifications of this bridge, a rubber-type seismic isolator with a lead core was added to it based on the Ashto standard. Two structural models were subjected to dynamic loads using incremental dynamic analysis. First, the Tebes record was applied incrementally to the structure and various seismic parameters were investigated in it. Next, the IDA and fragility curves of this structure were calculated and presented under twenty seismic records. The summary of the results is as follows:

- The study of the horizontal displacement of the superstructure under seismic loads showed that the horizontal displacement of the superstructure in the structure with the seismic isolator was greater than that of the initial structure. For example, in the Tebes earthquake record, the maximum horizontal displacement values in the superstructure of the bridge with seismic isolation at maximum accelerations of 0.1, 0.3, 0.5, 0.7, 0.9, 1.1 and 1.3 g were calculated to be 0.006, 0.019, 0.06, 0.13, 0.24, 0.34 and 0.45 m, respectively. These values in the original structure were calculated to be 0.006, 0.018, 0.05, 0.12, 0.22, 0.33 and 0.42 m, respectively.

- The study of the horizontal displacement of the column head shows that despite the increase in horizontal displacement in the superstructure with seismic isolation, the horizontal displacement value of the column and, as a result, the column drift values in the structure without seismic isolation were lower than in the original structure. For example, under the record of the Tebes earthquake, the maximum horizontal displacement values at the head of the bridge column with seismic isolation at maximum accelerations of 0.1, 0.3, 0.5, 0.7, 0.9, 1.1 and 1.3g have been calculated to be 0.00013, 0.009, 0.03, 0.04, 0.05, 0.1 and 0.14 m, respectively. These values in the original structure have been calculated to be 0.001, 0.01, 0.03, 0.09, 0.21, 0.3 and 0.39 m, respectively.
- The hysteresis curves of the moment of rotation in the columns of the two main structures and the structure equipped with a seismic isolator show that firstly, the bridge column in the structure with a seismic isolator enters the nonlinear region at higher maximum accelerations than the main structure, and also the width of the hysteresis curve in the structure with a seismic isolator is less than that of the main structure.
- The results show that despite the reduction in the dynamic response in the columns of the structure with a seismic isolator, in the superstructure section, the number of truss elements that have crossed the LS level at

some maximum accelerations in the structure with a seismic isolator was greater than that of the main structure.

- Examination of the fragility curves in the main structure and the structure with seismic isolation shows that in the three performance levels IO, LS and CP, the probability of failure in the column of the structure with seismic isolation was lower than that of the main structure. For example, in the IO performance level, the probability of failure at the maximum acceleration g_1 for the column of the isolated structure and the original structure was calculated to be 0.4 and 0.63, respectively. These values were calculated for the LS levels to be 0.18 and 0.39, respectively. Also, the probability of failure at the CP level at the maximum acceleration g_2 for the column of the isolated structure and the original structure was calculated to be 0.33 and 0.46, respectively. Therefore, it can be concluded that the use of seismic isolation in the Takab Bridge, despite reducing damage to the columns, can cause increased damage to the superstructure and truss elements.

8. References

- [1] Hosseinlou, F., Moradi, M., Sadrianzade, M., & Jalali, P. (2025). An energy-based method for calculating the fragility curve of bridges: a case study. *Iranian Journal of Science and Technology, Transactions of Civil Engineering*, 1-26.
- [2] Moradi, M., & Tavakoli, H. (2020). Proposal of an energy based assessment of robustness index of steel moment frames under the seismic progressive collapse. *Civil Engineering Infrastructures Journal*, 53(2), 277-293.
- [3] Azizinamini, A., Full scale testing of old steel truss bridge. *Journal of constructional steel research*, 2002. 58(5-8): p. 843-858.
- [4] Mousavi, A.A., et al., Structural damage localization and quantification based on a CEEMDAN Hilbert transform neural network approach: a model steel truss bridge case study. *Sensors*, 2020. 20(5): p. 1271.
- [5] Zhou, X., et al., Vibration-based Bayesian model updating of an actual steel truss bridge subjected to incremental damage. *Engineering Structures*, 2022. 260: p. 114226.
- [6] Pham, N.V., et al., Seismic Retrofit of Diagonal Tension Members in Steel Deck-Truss Bridges Using CFRP Sheets. *Journal of Composites for Construction*, 2023. 27(3): p. 04023023.
- [7] Chen, X., et al., Performance-Based Retrofits of Long-Span Truss Bridges Based on the Alternate Load Path Redundancy Analysis. *Journal of Bridge Engineering*, 2023. 28(2): p. 04022141.
- [8] Sosorburam, P. and E. Yamaguchi, Seismic retrofit of steel truss bridge using buckling restrained damper. *Applied Sciences*, 2019. 9(14): p. 2791.
- [9] Hanai, T., T. Tamura, and Y. Hirayama, Seismic retrofit of truss bridge for highway and railway, in *Maintenance, Safety, Risk, Management and Life-Cycle Performance of Bridges*. 2018, CRC Press. p. 1944-1950.
- [10] Li, S., et al., Performance-based seismic loss assessment of isolated simply-supported highway bridges retrofitted with different shape memory alloy cable restrainers in a life-cycle context. *Journal of Intelligent Material Systems and Structures*, 2020. 31(8): p. 1053-1075.
- [11] Deb, S.K., Seismic base isolation—An overview. *Current Science*, 2004: p. 1426-1430.
- [12] Yang, Y., L. Lu, and J. Yau, Structure and equipment isolation, in *Vibration and Shock Handbook*. 2005, CRC Press. p.

- 22.
- [13] Moradi, M., Tavakoli, H., & Abdollahzadeh, G. R. (2022). Collapse probability assessment of a 4-Story RC frame under post-earthquake fire scenario. *Civil Engineering Infrastructures Journal*, 55(1), 121-137.
- [14] Kulicki, J.M. Past, Present, and Future of Load and Resistance Factor Design-AASHTO LRFD Bridge Design Specifications. in 6th International Bridge Engineering Conference. 2005.
- [15] Bridges, S.o., S. Staff, and T.O.S.o. Bridges, Guide specifications for seismic isolation design. 2010: AASHTO.
- [16] Mojiri, S., W.W. El-Dakhkhni, and M.J. Tait, Seismic fragility evaluation of lightly reinforced concrete-block shear walls for probabilistic risk assessment. *Journal of Structural Engineering*, 2015. 141(4): p. 04014116.
- [17] Moradi, M. and M. Abdolmohammadi, Seismic fragility evaluation of a diagrid structure based on energy method. *Journal of Constructional Steel Research*, 2020. 174: p. 106311.
- [18] Moradi, M., Tavakoli, H., & Abdollahzade, G. (2024). Probabilistic evaluation of failure time of reinforced concrete frame in post- earthquake fire scenario. *Structural Concrete*, 25(5), 3487-3504.
- [19] Goodarzi, M. J., Moradi, M., Jalali, P., Abdolmohammadi, M., & Hasheminejad, S. M. (2023). Fragility assessment of an outrigger structure system based on energy method. *The Structural Design of Tall and Special Buildings*, 32(11-12), e2017..
- [20] Moradi, M., H. Tavakoli, and G. AbdollahZade, Sensitivity analysis of the failure time of reinforcement concrete frame under postearthquake fire loading. *Structural Concrete*, 2020. 21(2): p. 625-641.
- [21] Tavakoli, H. and M.M. Afrapoli, Robustness analysis of steel structures with various lateral load resisting systems under the seismic progressive collapse. *Engineering Failure Analysis*, 2018. 83: p. 88-101.
- [23] Li, S. Q., Liu, H. B., Farsangi, E. N., & Du, K. (2025). Seismic fragility estimation considering field inspection of reinforced concrete girder bridges. *Structure and Infrastructure Engineering*, 21(2), 302-318.
- [24] de Silva, D., Miano, A., De Rosa, G., Di Meglio, F., Prota, A., & Nigro, E. (2025). Analytical fire fragility assessment for bridges considering fire scenarios variability. *Engineering Structures*, 325, 119442.
- [25] Lian, Q., Chen, L., Dang, X., Zhuo, W., & Li, C. (2025). Dynamic response and fragility of mountain bridges under the coupled effects of transverse earthquakes and landslides. *Soil Dynamics and Earthquake Engineering*, 188, 109079.
- [26] Yan, B., Lai, J., Wu, S., Feng, S., & Meng, X. (2025). Seismic fragility assessment of UHPC ribbed arch bridges. *Soil Dynamics and Earthquake Engineering*, 190, 109199.
- [27] Kumar, V., Singh, V., & Shekhar, S. (2025). Mainshock-Aftershock Ground Motion Sequences Selection and its Implication on Bridge Seismic Fragility. *Journal of Earthquake Engineering*, 1-24.